Physicochem. Probl. Miner. Process., 55(1), 2019, 268-277

http://www.journalssystem.com/ppmp

Physicochemical Problems of Mineral Processing

ISSN 1643-1049

Received February 17, 2018; reviewed; accepted May 9, 2018

Study on feature extraction and dynamic properties of bubbles in a liquid-phase flow field

Deqiang Peng [1, 2], Xianshu Dong [1], Yuping Fan [1], Xiaomin Ma [1]

[1] College of Mining Engineering, Taiyuan University of Technology

[2] School of Mining Engineering, Heilongjiang University of Science and Technology

Corresponding author: dongxsh520@163.com (Xianshu Dong)

Abstract: To study the dynamic properties of bubbles generated at different air pressures in a liquid-phase flow field, this paper adopted high-speed camera technology and image processing techniques to extract and calculate the features of bubbles. The results showed that in a deionized water field, the bubbles generated at the air pressure of 0.1 MPa had an average diameter of 4.50 mm, and the bubbles generated at the air pressures of 0.2 MPa and 0.3 MPa had average diameters of 5.74 mm and 5.76 mm respectively; notwithstanding the insignificant differences in average data, the probability distribution of bubble diameter had significant differences with different pressures. During the rise of bubbles, their motion trajectory witnessed an increased amplitude of swing with the increase of air pressure; the bubbles generated at different air pressures did not show any significant differences in rising velocities though.

Keywords: bubbles, image processing, trajectory, probability distribution of diameter, terminal velocity

1. Introduction

In modern industry, two-phase flows play an increasingly important role (Fan et al., 2009) in many fields, including distillation towers, wastewater treatment, petrochemical engineering and mineral flotation (Liu et al., 2005; Yang et al., 2006; Liu et al., 2006; Saito et al., 2006). These problems are closely related to the dynamic properties of bubbles, so studying the shape and motion of gas bubbles in fluids is of vital theoretical significance for solving practical engineering problems (Yan et al., 2016). The main dynamic features of bubbles involved in two-phase interactions include size, shape, velocity and so forth of bubbles, which have been explored to varying degrees throughout both modelling and experiments.

There are several effect factors on bubbles generating in the liquid. Pressure, gas flow rate and liquid phase are the main factors. Suresh and Mania (2012) mainly focused on the influence of gas flow on bubble shape, and the results indicated that with an increased gas flow, bubble shape gradually changes from spherical to hemispherical and spherical cap shape. Lesage and Marios (2013) explored the correlations of bubble departure volume with gas flow, nozzle bore and bubble shape. Guo et al. (2009) adopted high-speed CCD imaging technology to experimentally determine the deformation properties and rising terminal velocity of single bubbles in water and in glycerin solutions of different viscosities, and the experimental results showed that small bubbles where generally all spherical shaped even with the increase of liquid-phase viscosity, and that large bubbles gradually changed from an irregular ellipsoid shape to spherical cap shape. The gas flow rate in the literature that influenced the shape and size of bubbles is at a constant pressure.

The influence of pressure on the bubble rise has also been studied. Luo et al. (1997) have studied the effect of external pressure on bubble rise velocity. Letzel (1998) has systematically analyzed the effect of gas density on the rise velocity of large bubbles. But the research on the pressure mainly focused on the

DOI: 10.5277/ppmp18128

external pressure in the column (Kulkarni and Joshi, 2005). Few literature sources mentioned the effect of jetting pressure.

The terminal velocities and the trajectory of rise bubbles have been studied for the theoretical prediction and experimental test. Peters and Els (2012), through performing an experimental study on bubbles in motion in tap water, drew the conclusion that the motion velocity of bubbles is closely correlated with their shape and surface oscillation (Yan et al., 2016). Amirnia et al. (2013) use a high-speed camera to investigate the rising process of bubbles in liquid, and the experimental results showed that bubbles in liquid linearly rise when their diameter was relatively low, and that, with the increase of diameter, their path become more irregular. Zhang et al. (2008) studies the correlation between the accelerated motion of single bubbles in liquids of different viscosities and their drag coefficients. Raymond and Rosant (2000) experimentally studied the rising behavior of bubbles in different viscosity systems, and obtained the correlation of Reynolds number with the drag coefficient. Zhang et al. (2013) conducted experiments to investigate the behavioral properties of single bubbles rising in a vertical uniform channel, traced the changes in their motion trajectory and shape throughout this process, and determined the formula of the drag coefficient throughout the rising process of bubbles. Gu and GUO experimentally studied the morphological features of single bubbles in gas-liquid two-phase flows within horizontal pipes and downward inclined pipes, and determined the relation between bubble velocity and the Froude number (Gu et al., 2006; Gu and Guo, 2008). Kulkarni and Joshi (2005) has reviewed the bubble formation and bubble rise velocity in gas-liquid systems. The investigators mainly focus on a single bubble velocity in the studies. However, the velocity and size of chain bubbles, pairing bubbles or bubble swarms are needed to study furthermore.

This paper uses a high-speed camera and image-processing to extract the various parameters of chain bubbles generated at different air pressures to determine the changes in diameter, motion trajectory and rising velocity with the change in air pressure.

2. Material and methods

2.1. Experimental setup

The experimental setup mainly consists of three parts: I) image acquisition and processing system; II) experimental observation system; III) aerodynamic system, as shown in Fig. 1. The image acquisition & processing system was mainly composed of a high-speed camera and image processing software. The high-speed camera was used to take a group of images 2,048x2,048 in pixel size. The images acquired under parallel light were then subject to image identification and calculation by SimplePCI Software, and statistics were made of the feature values of the bubbles.

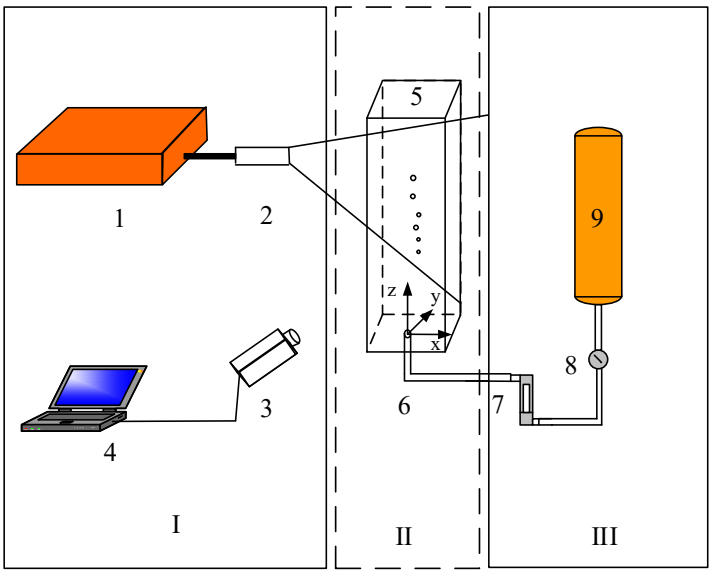

Fig. 1. Schematic of experimental setup. 1 - light source; 2 - light; 3 - camera; 4 - computer; 5 - visual column; 6 - orifice; 7 - flowmeter; 8 - manometer; 9 - compressor

The experimental observation system was composed of an observation chamber and inflation inlet. The observation chamber was 400 mm in length and width, and 600 mm in height, and made of acrylic. The inflation hole had medical needle tubing with an inner diameter of 0.6 mm fixed at the bottom center of the observation chamber.

The aerodynamic system was composed of an air compressor (Shengkai, China), pressure gauge and flow meter. The pressure tank had a volume of 30×10^{-3} m^3, and can consistently output air pressures from 0~0.8 MPa.

2.2. Experimental conditions

In the experiment, the liquid phase was deionized water, with the density of 998 kg/m^3 and the viscosity of 1×10^{-3} Pa·s. The gaseous phase was compressed air, with a density of 1.205 kg/m^3 and a viscosity of 0.1818×10^{-3} Pa·s. The air pressures were respectively 0.1 MPa, 0.2 MPa and 0.3 MPa. For the convenience of observing the motion of bubbles in the liquid phase, the experiment used parallel light irradiation.

3. Feature value extraction of bubbles

See the images acquired in the experiment in Fig. 2-a. The series of images acquired were first put through preprocessing, and then subject to subsequent processing by SimplePCI Software. The processing procedure included four steps: 1) the luminance threshold was adjusted to identify bubble contours in the images, as shown in Fig. 2-b; 2) the contours were then filled in; 3) the pixels in the filling zone were then counted, and statistics the diameter, centroid position, circularity and other information within the contoured areas were calculated; 4) finally, identification data was matched with the bubbles to obtain the feature value of each bubble, as shown in Fig. 2-c.

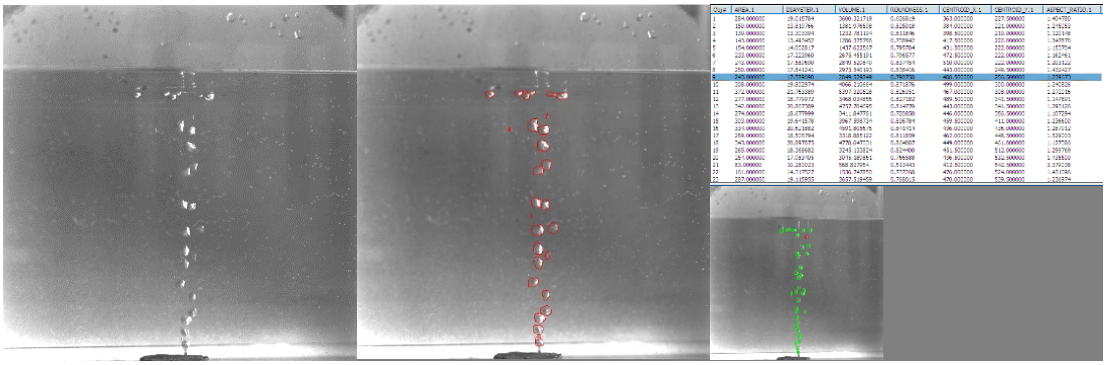

a b c

Fig. 2. Bubble feature extraction. a. original images; b. bubble contour recognition; c. the recognition data match of the bubble contour

The algorithm used to identify and calculate the various parameters followed these steps:
1) Pixel point marking

$$P_i = \begin{cases} 0 & L < L_0 \\ 1 & L > L_0 \end{cases} \tag{1}$$

where L_0 was the threshold of image background, L- threshold of image pixel point; P_i - marked pixel point.
In this case, the bubble area would be:

$$A_i = \sum_{i=1}^{n} P_i \tag{2}$$

where A_i represents the bubble area, pix^2.

According to the relationship between the area and diameter, the equivalent diameter of bubbles can be obtained by:

$$d_i = 2\sqrt{\frac{A_i}{\pi}} \tag{3}$$

where d_i represents the equivalent diameter of bubbles in pixels.

4. Results and discussion

4.1. Area and equivalent diameter of bubbles

When measuring the parameters of bubbles in the liquid phase, generally the bubble volume and diameter are used to characterize bubble size. Modeling is typically used to calculate bubble volume as bubbles may not be perfectly round, and calculation models were selected here according to the different bubbles generated throughout the experiments (GUO et al., 2009). This method required the artificial judgment of bubble shape and the artificial selection of the proper calculation formula, so the steps were tedious. To accelerate the process of bubble size calculation, this paper used image processing software to identify the bubble area and further determine the bubble diameter. Fig. 3 depicts the equivalent diameter distribution relationship of bubbles at different vertical heights. As can be seen from Fig. 3, the diameter of the bubbles generated at the same air pressure had no significant trend with their height in the liquid-phase environment. However, with the change in air pressure, bubble diameter increased. The diameter of bubbles generated at 0.1 MPa was smaller than both the diameter of the bubbles generated at 0.2 MPa and that of bubbles generated at 0.3 MPa. However, there was no significant diameter difference between bubbles generated at 0.2 MPa and those generated at 0.3 MPa.

For the purpose of further determining the relationship between the bubble diameter and air pressure, the bubbles generated at air pressures of 0.2 MPa and 0.3 MPa were then ranked by diameter size, and average bubble diameters were calculated as well, as shown in Table 1. Fig. 4 shows the equivalent diameter relationship among bubbles generated at different air pressures. When the air pressure was less than 0.3 MPa, the diameter of the bubbles increased with the increase of air pressure. According to the data in Tab.1, the bubbles generated at an air pressure of 0.2 MPa and those generated at an air pressure of 0.3 MPa were essentially equivalent in average diameter.

Table 1. The bubble mean equivalent diameter

Air pressure /MPa	Gas flow rate /10^{-5} m^3/s	Bubble mean equivalent diameter/mm
0.1	1.33	4.50
0.2	1.67	5.74
0.3	2.0	5.76

4.2. Probability distribution of bubble diameter

Bubble size is an important parameter, and one of the three parameters (the other two being gas holdup and gas flow velocity) which jointly determine the dispersion of gas in a liquid (Grau and Heiskannen, 2005). Throughout the flotation process, bubble size and uniformity exert an influence on the form of mineralization. Thus, investigating bubble diameter distribution is of vital significance for studies on flotation behavior.

To better judge the diameter relations of bubbles generated at different air pressures, this paper cites the probability distribution of bubbles to characterize the status of bubble diameter distribution.

This study calculated the statistics of the equivalent diameter of bubbles, and used the interval of 1mm to count the frequency of bubbles within that diameter range. Then, the statistics of this bubble number was transformed into the probability density function of bubble diameter. See the statistics of bubble diameter probability distribution at different air pressures in Fig. 5. As can be seen from the curves shown Fig. 5, the distribution of bubble diameter was concentration in for a particular size range for each air pressure in a Gaussian curve. The peak of bubble diameter distribution at the air pressure of 0.1 MPa occurred at about 4.5 mm, with a probability density of 0.4; at air pressures of 0.2 MPa and 0.3 MPa, the peaks occurred at about 6.0 mm, with their probability densities respectively being 0.3 and 0.2. The peaks here show some deviations from the average equivalent diameter of bubbles shown in Table 1, that is, the higher the air pressure, the more significant the deviation.

Peak size represents the density of bubbles near a peak, that is, the higher the peak, the more the bubbles with that diameter. Peak width represents the dispersion degree of bubble size, that is, the

greater the peak width, the wider the bubble diameter range. A smaller peak width corresponds to a narrower bubble diameter range. According to curve analysis, the particle size distribution of the bubbles was presented in different states for the different air pressure intervals. Combined with the data in Fig. 4, the diameters of bubbles generated at 0.1 MPa were mainly concentrated around 4.5 mm, and that the bubbles are relatively uniform in size and shape. When the air pressure ranged between 0.2 MPa and 0.3 MPa, the bubble diameter data obtained through identification had a relatively wide distribution range, so there are certain deviations between the average equivalent diameter of bubbles and their density distribution.

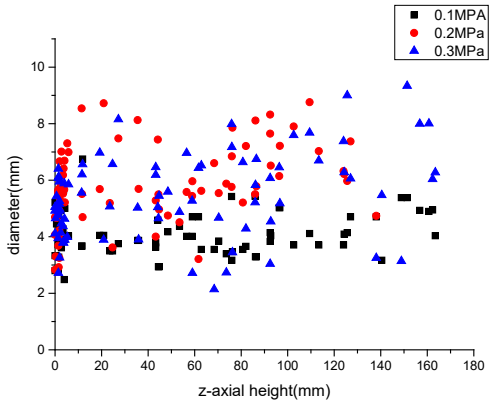

Fig. 3. Bubble distribution in the z-axial height

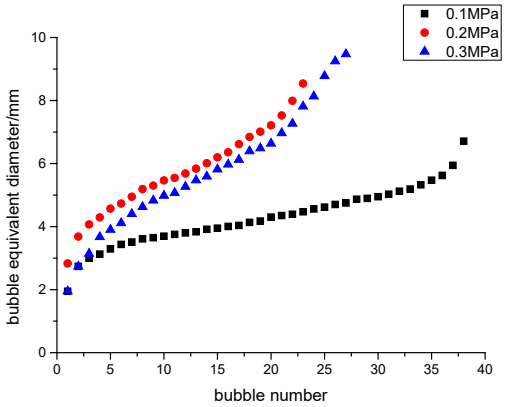

Fig. 4. The influence of air pressure on the bubble equivalent diameter

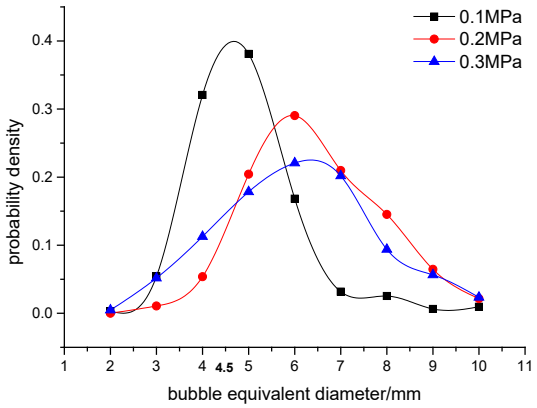

Fig. 5. The probability distribution of bubble diameter

4.3. Effect of pressure on the bubble diameter

There are many formulas to calculate the bubble diameter or bubble volume when the bubble formats at submerged orifice, e.g. Single stage model or two stage model (Kulkarni and Joshi, 2005). The bubble diameter can get by Tale's law in the quasi-static liquid. The formula is

$$V_d = \frac{2\pi\sigma}{(\rho_L - \rho_{air})gb^2} \tag{4}$$

where, b is the diameter is ca.3.1mm according to the Tate's law (Tate, 1864; Lesage and Marois, 2013). However, the experimental dates showed the bubble diameter has a wide range. The reason is that chain bubbles generate in the experiment and cause the liquid around the bubble moves with some speed. Therefore, when the chain bubbles rise, the diameter should be calculated by the pressure equation (5) (Terasaka et al., 1999),

$$P_B - P_H = \rho_L \left[R\frac{d^2R}{dt^2} + \frac{3}{2}\left(\frac{dR}{dt}\right)^2 + \frac{V_L^2}{2} \right] + \frac{2\sigma}{R} + \frac{4\mu_L}{R}\frac{dR}{dt} \tag{5}$$

where, P_H, ρ_L, σ, μ_L,V_L are static liquid pressure at any element, liquid density, surface tension, viscosity and liquid velocity, respectively. P_B is the pressure in bubble and equels to the air pressure P_{air} before the bubble goes away from the orifice. When P_{air} increases, the bubble diameter increases until it is up to a maximum value. The value is determined by σ. And when the P_{air} is constant, the V_L influents on the bubble diameter. So the bubble diameters has a wide range.

4.4. Motion trajectory of bubbles

In a liquid-phase environment, bubbles are engaged in three types of motion during their rise: linear, zigzag and spiral. To investigate the motion trajectories of the bubbles during their rise at different air pressures, this paper traced the rising bubbles, using image processing software to calculate statistics of the centroid position of the bubbles, adopted mapping software to delineate their relative positions and introduced curves for coupling purpose. The motion trajectory chart of bubbles in Fig. 6 is obtained. As can be seen from Fig. 6, with the increase of air pressure, the motion trajectory of the bubbles presented a widened range of fluctuation. At an air pressure of 0.1 MPa and a height of less than 120 mm, bubbles were engaged in a linear rising trajectory; when the height exceeded 120 mm, bubbles were engaged in a zigzag motion; when the air pressure was 0.2 MPa, bubble rise was almost dominated by once again by a linear rise; when the air pressure was 0.3 MPa, bubbles departed from the pipe orifice and begin to ascend in a zigzag motion.

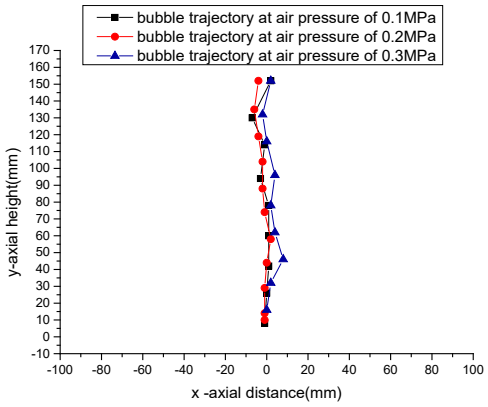

Fig. 6. The trajectory of bubble rising in the liquid

4.5. Motion velocity of bubbles

When the bubbles departed from the pipe orifice and move upwards, their motion velocity was solved according to the definition of velocity. In this paper, velocity was calculated through continuously tracing and shooting the same bubble and measuring its different displacements. Fig. 7 depicts the motion velocities of bubbles at different air pressures. As can be seen from the data in Fig. 7, the motion velocities in the liquid phase of bubbles generated at different air pressures showed little difference, and the average velocities of the bubble motion fell within the range of 0.32~0.39 m/s. When bubbles

departed from the pipe orifice by a distance of 30 mm, the bubble velocities essentially reached their peak. Fig. 8 and Fig. 9 respectively provide the components of the bubble ascending velocity in the horizontal direction and vertical direction. In the ascending process, the velocity range of bubbles in the horizontal direction was -0.2 m/s~0.2 m/s.

Table 2. Terminal velocity prediction models for bubble motion

Investigator	Formula	Applicable conditions
Mandelson (1967)	$V_T = \sqrt{g r_B + \frac{\sigma}{r_B \rho_l}}$	Applicable to liquid-phase environment of medium particle size (>2mm)
Nickens and Yannitell (1987)	$V_T = 0.361(1 + \frac{4.89}{E_0})^{0.25}$ $E_0 = \frac{g(\rho_L - \rho_{air}) d_{eq}^2}{\sigma}$	Applicable to the Air-Newtonian liquid over wide range of properties

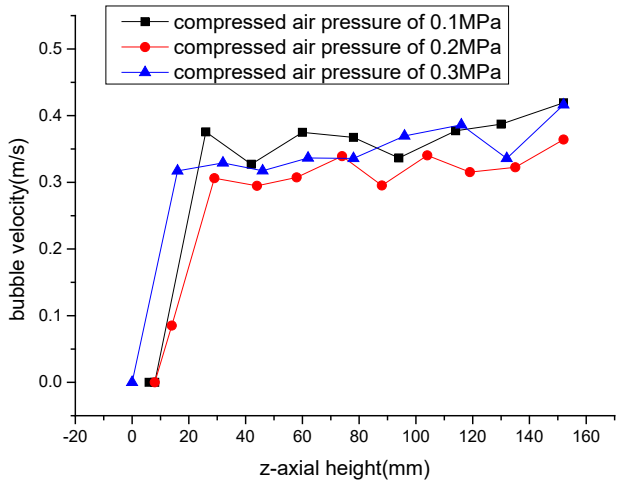

Fig. 7. The bubble velocity in the z-axial height

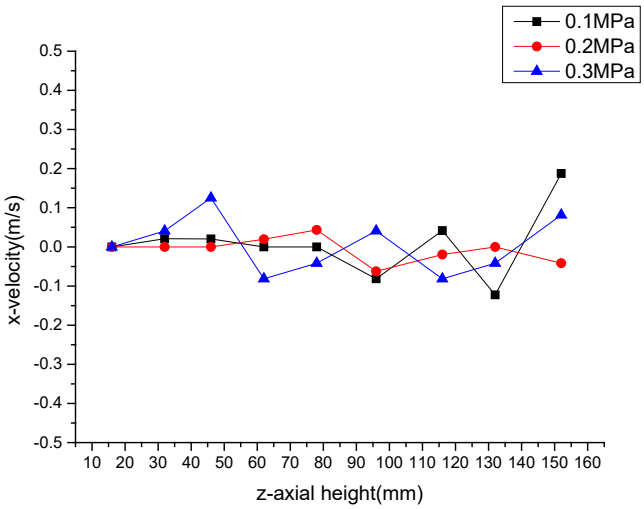

Fig. 8. X-velocity in the z-axial height

Although the conclusion has drawn that the experimental velocity of bubble generated at different air pressure is almost same, as shown from Fig. 7 to Fig. 9. But the relationship between bubble diameter and terminal velocity need to be for a further study. So, the experimental velocity statistics of bubbles which diameters range from 4.1 mm to 7.8 mm are obtained, as is shown in Fig. 10. Furthermore, the paper compared the experimental rising velocity with the terminal velocity which calculated by the prediction models for bubble motion. The prediction models include Mandelson's formula (Mendelson, 1967) and Nickens' formula (Nickens and Yannitell, 1987), which are listed in Table 2 (Kulkarni and Joshi, 2005). The terminal velocities of bubble are calculated by Mendelson's formula, which are lower than the experimental velocity (Fig. 10) and can not predict the actual velocity. While, the trend of velocities calculated by Nickens' formula comes to reach the experimental velocities. And the terminal velocities keep stable when the diameters are above 7.0 mm, so it can use the Nickens' formula to predict the actual rising velocity.

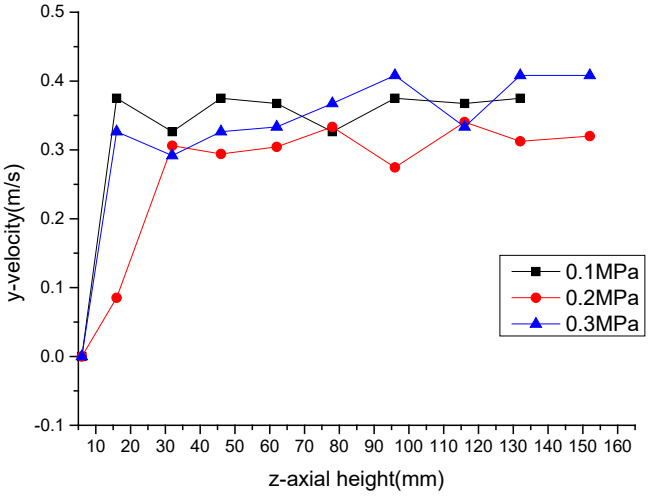

Fig. 9. The y-velocity in the z-axial height

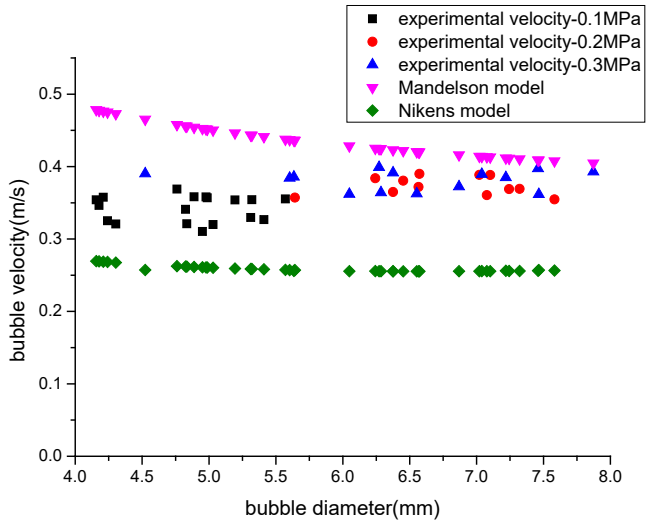

Fig. 10. Bubble terminal velocity – comparison between theory and experiment

5. Conclusions

This paper experimentally investigated the properties of bubbles generated in deionized water at different air pressures, and the following can be concluded:

(1) In deionized water, when the air pressure is less than or equal to 0.3 MPa, the diameter of the bubbles generated increases with the increase of air pressure; the bubbles generated at an air pressure

of 0.1 MPa had an average diameter of 4.50 mm, and the bubbles generated at an air pressures of 0.2 MPa and 0.3 MPa had similar values, with average diameters of 5.74 mm and 5.76 mm, respectively; it is true that the average diameters of the bubbles generated at 0.2 MPa and 0.3 MPa were approximate, but, seen from the probability distribution of the bubble diameter, the diameters of bubbles generated at 0.2 MPa were relatively concentrated, while those of bubbles generated at 0.3 MPa showed more significant fluctuations.

(2) During bubble rise, with the increase of air pressure, the motion trajectory of the bubbles fluctuates more and more significantly.

(3) During bubble ascension, the bubbles generated at different air pressures do not show any significant differences in average velocities. In comparison to the theoretically calculated velocities, the data measured in the experiment were closer to the values calculated by Nickens' formula when the bubble diameters are above 7.0 mm.

Acknowledgments

This research was supported by National Natural Science Foundation of China under agreement number 51604189 and 51674174. The research was also supported by Natural Science Foundation of Shanxi Provence under agreement number 201601D011056.

References

AMIRNIA, S., BRUYN, J. R. D., BERGOUGNOU, M. A., MARGARITIS, A., 2013. *Continuous rise velocity of air bubbles in non-Newtonian biopolymer solutions*, Chemical Engineering Science 94(5), 60−68.

FAN, W., MA, Y., LI, X., LI, H., 2009. *Study on the flow field around two parallel moving bubbles and interaction between bubbles rising in CMC solutions by PIV*, Chinese Journal of Chemical Engineering 17(6), 906-913.

GRAU, R. A., HEISKANEN, K., 2005. *Bubble size distribution in laboratory scale flotation cells*, Minerals Engineering 18, 1164-1172.

GU, H., GUO, L., 2008. *Shape of Isolated Bubble in Downwardly Inclined Gas-Liquid Two-phase Flows*, Nuclear Power Engineering 29, 30-34.

GU, H., GUO, L., ZHANG, X., WANG, Z., 2006. *The shape of isolated bubble in Intermittent flows in horizontal straight tube*, Journal of engineering thermophysics 27, 433-436.

GUO, R., CAI, Z., GAO, Z., 2009. *The Motion Characteristics of a Single Bubble in Stagnant Highly Viscous Liquids*, Journal of Chemical Engineering of Chinese Universities 23, 916-921.

HABBERMAN, W. L., MORTON, R. K., 1953. *An experimental investigation of the drag and shape of air bubbles rising in various liquids*, Navy Department Report 802, Washington D.C., 1-47.

JAMIALAHMADI, M., BRANCH, C., MULLER-STEINHAGEN, H., 1994. *Terminal bubble rise velocity in liquids*, Chem. Eng. Res. Des. 72(A), 119-122.

KULKARNI, A. A., JOSHI, J. B., 2005. *Bubble formation and bubble rise velocity in gas-liquid systems: a review*, Ind. Eng. Chem. Res. 44, 5873-5931.

LESAGE, F. J., MARIOS, F., 2013. *Experimental and numerical analysis of quasi-static bubble size and shape characteristics at detachment*, International Journal of Heat and Mass Transfer 64(3), 53−69.

LETZEL, M., 1998. *Hydrodynamics and mass transfer in bubble columns at elevated pressures*, Ph. D. Thesis. Delft University.

LIU, Z., ZHENG, Y., 2006. *PIV study of bubble rising behavior*, Powder Technology 168, 10-20.

LIU, Z., ZHENG, Y., JIA, L., ZHANG, Q., 2005. *Study of bubble induced flow structure using PIV*, Chemical Engineering Science 60, 3537-3552.

LUO, X., ZHANG, J., TSUCHIYA, K., FAN, L., 1997. *On the rise velocity of bubbles in liquid-solid suspensions at elevated pressure and temperature*, Chem. Eng. Sci. 52(21-22), 3693.

MENDELSON, H. D., 1967. *The prediction of bubble terminal velocities from wave theory*, AIChE J. 13, 250-253.

NICKENS, H. V., YANNITELL, D. W., 1987. *The effects of surface tension and viscosity on the rise velocity of a large gas bubble in a closed vertical liquid-filled tube*, Int. J. Multiphase Flow 13(1), 57-69.

PETERS, F., ELS C.., 2012. *An experimental study on slow and fast bubbles in tap water*, Chemical Engineering Science 82(1), 194−199.

RAYMOND, F., ROSANT, J. M., 2000. *A numerical and experimental study of the terminal velocity and shape of bubbles in viscous liquids*, Chem. Eng. Sci. 55(5), 943-955.

SAITO, T., SAKAKIRBARA, K., MIYAMOTO, Y., YAMADA, M., 2006. *A study of surfactant effects on the liquid-phase motion around a zigzagging-ascent bubble using a recursive cross-correlation PIV*, Chemical Engineering Journal 158, 39-50.

SURESH, M., MANI, A., 2012. *Experimental studies on bubble characteristics for R134a–DMF bubble absorber,* Experimental Thermal and Fluid Science 39, 79−89.

TATE, T., 1864. *On the magnitude of a drop of liquid formed under different circumstances*, Philos. Mag. 27, 176–180.

TERASAKA, K., TSUGE, H., MATSUE, H., 1999. *Bubble formation in co-currently upward flowing liquid*. Can. J. Chem. Eng. 77, 458-464.

YAN, H., ZHAO, G., LIU, L., DUAN, J., 2016. *Experimental study on shape and rising behavior of single bubble in stagnant water*, Journal of Central South University (Science and Technology) 47, 2513-2520.

YANG, G. Q., DU, B., FAN, L. S., 2006. *Bubble formation and dynamics in gas-liquid-solid fluidization - A review*, Chemical engineering science 62, 2-27.

ZHANG, L., YANG, C., MAO, Z., 2008. *Unsteady motion of a single bubble in highly viscous liquid and empirical correlation of drag coefficient,* Chem. Eng. Sci. 63(8), 2099-2106.

ZHANG, Y., NI, J., LI, W. Z., 2013. *Experimental study on a single bubble rising in a vertical wedge-shaped channel*, Journal of Experiments in Fluid Mechanics 27, 50-56.